IEEE Access
Multidisciplinary | Rapid Review | Open Access Journal

Received December 13, 2021, accepted January 23, 2022, date of publication January 28, 2022, date of current version February 8, 2022.

Digital Object Identifier 10.1109/ACCESS.2022.3147672

Multi-Objective Optimization of PV and Energy Storage Systems for Ultra-Fast Charging Stations

CAROLA LEONE[1], MICHELA LONGO[1], (Member, IEEE), LUIS M. FERNÁNDEZ-RAMÍREZ[2], (Senior Member, IEEE), AND PABLO GARCÍA-TRIVIÑO[2]

[1]Department of Energy, Politecnico di Milano, 20156 Milan, Italy
[2]Research Group in Sustainable and Renewable Electrical Technologies, Department of Electrical Engineering, Higher Technical School of Engineering of Algeciras (ETSIA), University of Cádiz, 11202 Cádiz, Spain

Corresponding author: Carola Leone (carola.leone@polimi.it)

ABSTRACT The installation of ultra-fast charging stations (UFCSs) is essential to push the adoption of electric vehicles (EVs). Given the high amount of power required by this charging technology, the integration of renewable energy sources (RESs) and energy storage systems (ESSs) in the design of the station represents a valuable option to decrease its impact on the grid and the environment. Therefore, this paper proposes a multi-objective optimization problem for the optimal sizing of photovoltaic (PV) system and battery ESS (BESS) in a UFCS of EVs. The proposed multi-objective function aims to minimize, on one side, the annualized cost of the station, and on the other side, the produced pollutant emissions. The decision variables are the number of PV panels and the capacity of the ESS to be installed. The optimization problem is reduced to a single-objective problem by applying the linear scalarization method. Then the equivalent single-objective function is optimized through a genetic algorithm (GA). The proposed optimization framework is applied to a study case and the results prove that PV and ESS could lead to a significant reduction of both the annualized cost and the pollutant emissions. Finally, a sensitivity analysis is also presented to validate the effectiveness of the proposed solution.

INDEX TERMS Extreme fast charging, integrated charging station, bi-objective optimization, electric vehicles, fast-charging load demand.

NOMENCLATURE

ACRONYMS

EV	Electric Vehicle.
UFC	Ultra-Fast Charging.
UFCS	Ultra-Fast Charging Station.
ICE	Internal Combustion Engine.
PV	Photovoltaic.
RES	Renewable Energy Sources.
ESS	Energy Storage System.
BESS	Battery Energy Storage System.
COE	Cost of Electricity.
NPV	Net Present Value.
LCC	Life Cycle Cost.
LPSP	Loss of Power Supply Probability.
MILP	Mixed-Integer Linear Programming.
MOPSO	Multi-Objective Particle Swarm Optimization.
GA	Genetic Algorithm.
LCOE	Levelized Cost of Electricity.
CFOE	Carbon Footprint of Electricity.
NWCMO	Normalized Weighted Constrained Multi-Objective.
SoC	State of Charge.
V2G	Vehicle-to-Grid.
MV	Medium Voltage.
DC	Direct Current.
AC	Alternating Current.
DOD	Depth-Of-Discharge.
CRF	Capital Recovery Factor.
CO_2	Carbon dioxide.
SO_2	Sulphur dioxide.
NO_x	Nitrogen oxides.

The associate editor coordinating the review of this manuscript and approving it for publication was Moussa Boukhnifer.

This work is licensed under a Creative Commons Attribution 4.0 License. For more information, see https://creativecommons.org/licenses/by/4.0/

PARAMETERS

a	Weibull pdf scale factor.
b	Weibull pdf shape factor.
t	Instant of time.
P^*_{PV}	Output power of a single solar panel.
P_{PV}	Output power of the PV system.
P^r_{st}	Ideal output power a solar panel.
G	Irradiance.
G_{st}	Irradiance in standard condition.
δ	Derating factor of solar panel.
α	Temperature coefficient.
T_c	Cell temperature.
T_{st}	Cell temperature at standard conditions.
E_{BESS}	Battery energy.
σ	Battery self-discharge rate.
P_{grid}	Power provided by the grid.
CRF	Capital Recovery Factor.
E_{BESS}	Energy from/to the battery.
P^{ch}_{BESS}	Battery charging power.
η^{ch}_{BESS}	Battery charging efficiency.
P^{dis}_{BESS}	Battery discharging power.
η^{dis}_{BESS}	Battery discharging efficiency.
P^{dis}_{max}	Battery maximum discharging power.
P^{ch}_{max}	Battery maximum charging power.
E^{min}_{BESS}	Battery minimum allowed energy level.
E^{max}_{BESS}	Battery maximum allowed energy level.
λ_1, λ_2	Binary variables defining the direction of the energy in the battery.
AC_k	Annual cost of the k-th component.
AIC_k	Annualized capital cost of component k-th.
$AO\&M_k$	Annual operation and maintenance cost.
ARC_k	Annual replacement cost.
RV_k	Residual value.
N_k	Number of k-th component.
C_{grid}	Cost of the energy purchased from the grid.
i	Interest rate.
y	System lifetime.
$P_{grid}(t)$	Power absorbed from the grid.
E_{pr}	Electricity price.
E_{poll}	Pollutant emission.
e_{CO_2}	CO_2 emission factors.
e_{SO_2}	SO_2emission factors.
e_{NO_x}	NO_xemission factors.
w_i	Weight factors.

OPTIMIZATION VARIABLES

N_{PV}	Number of PV panels.
N_{BESS}	Number of BESS units.

I. INTRODUCTION

In recent decades, environmental concerns are gaining ever more interest worldwide. In this context, particular attention has been dedicated to the transport sector and conventional oil vehicles, because of their high CO_2 emissions and consequently footprint [1]. Many researchers, in these last years, have proved that the introduction of EVs is an effective way to reduce oil dependence and consequently decrease pollution [2], [3]. For all these reasons, the penetration of EVs is expected to grow exponentially over the next few years. To promote and support this electrification trend the installation of reliable and well-integrated charging stations is required.

In Italy, the number of publicly accessible AC charging points available in the country increased exponentially over the last five years, passing from 1,679 units in 2015 to 12,150 units in 2020 [4]. Nevertheless, these numbers do not take into account the extreme fast-charging systems, which become essential when medium and long-distance travels are concerned. Ultra-fast or extreme charging (UFC) systems have typical power rates between 50 kW up to 350 kW [5]. Therefore, compared to slow charging, UFC allows recharging the EV in times about 25-35 minutes. However, its biggest disadvantage is that of requiring large power demand, and hence, greatly impact on the national electric grid [6].

To mitigate this aspect, renewable energy sources (RES), and energy storage systems (ESS) can be incorporated into the design of UFCS. Indeed, if well-planned, the integration of wind turbines, PV panels, and ESS in the UFCS not only can reduce the grid and the environmental impacts but can also allow a lifespan cost reduction of the entire structure, knowing that this is one of the most critical aspects which opposes to the spread of this type of charging system [7]. However, to take advantage of the benefits coming from the integrated charging station, the design must be well-planned, as a matter of fact, on one side, too high RES and ESS capacities will lead to a waste of costs and resources, and on the other side, instead, a too low capacity which does not meet the load demand will not avoid the large flow of electricity from the public grid.

Several studies in the literature have focused on the development of charging infrastructure integrated with any sort of RES and ESS and how to optimally size these additional resources. The optimization problem of system sizing can be composed of one or more objective functions to be minimized, and the research can be divided into single-objective and multi-objective optimization.

In single-objective optimization usually, the objectives are related to the economic aspects, and the function to minimize can be represented by the following cost indicators: the cost of electricity (COE), the net present value (NPV), or the life cycle cost (LCC). For example, in [8], the authors proposed a single-objective optimization problem solved through a mixed-integer linear programming (MILP) algorithm, whose aim was to minimize the total energy costs of an ultra-fast charging station integrated by a BESS and PV system. Not only the size of PV panels and ESS but also the optimal size of a wind turbine was carried out in [9] for a stand-alone charging station, and in the objective function, the LCC

of the system is minimized through a hybrid optimization algorithm. Different from the above-mentioned literature, in [10], the optimal integration between the EV charging station and the RES was carried out based on reliability analysis. Indeed, the authors aim to enhance the reliability of the system by minimizing the energy not supplied to the customers.

If, in addition to the cost and economic indicators, other aspects would like to be included in the optimization problem, such as reliability and environmental benefits, then a multi-objective optimization must be performed. The main advantage of multi-objective optimizations is that they allow taking into consideration more criteria, and thus, provide more reliable and accurate results. However, when there are two or more objective functions in the problem, the calculation difficulty and times increase. To solve multi-objective optimization problems many algorithms have been used in literature. In [11] the optimal size for a stand-alone relay telecommunication station integrating PV/wind turbine and BESS was computed by using the concepts of loss of power supply probability (LPSP) and the annualized cost of the system. A GA was used to minimize the functions. In [12] instead, the optimization aimed to minimize both the COE and the environmental impact of an EV charging station with 10 piles and a maximum charging power for each pile of 40 kW. To solve the problem, a hybrid optimization algorithm joining the multi-objective particle swarm optimization (MOPSO) algorithm and technique for order preference by similarity to ideal solution (TOPSIS) method was used. A MOPSO algorithm was also applied in [13] to solve an optimization problem with COE and LPSP as objective functions. The model was then applied to a PV/wind/hydropower station with pumped storage and as load demand, the real absorption of the city of Xiaojin was used. The authors in [14] employed a hybrid GA-PSO algorithm to determine the optimal capacity of RES generation, and its optimal scheduling. The optimization function was composed of four objectives, however, any restriction about the charging power of EV was considered but only the overall energy required in one day. In [15], the final multi-objective function was composed of four objectives: LPSP, Levelized Cost of Electricity (LCOE), Carbon Footprint of Electricity (CFOE), and a socio-political objective. A weighted constrained multi-objective optimization algorithm (NWCMO) was implemented to obtain the optimal size of all the components inside the station. Table 1 provides the review of the most important studies presented above.

It is worth noting that in all the reported literature, only charging stations with a maximum charging rated power of 50 kW for each charging point have been considered. Moreover, the differences existing in the many EVs on the market are not taken into account. Therefore, to the best knowledge of the authors, the optimal design of a charging station integrating RES and ESS has never been extended to ultra-fast charging technology, which indeed is the purpose of this paper. Finally, in all the literature, the charging power limit imposed by the vehicle battery itself has never been taken into account.

TABLE 1. Review of optimal sizing of charging stations.

Ref.	Charging load	Objective Functions	Solution Method
[11]	-	LPSP, cost	GA
[12]	40kW for 10 poles	COE, Emission	MOPSO+ TOPSIS
[13]	Real demand of Xiaojin city	COE, LPSP	MOPSO
[14]	Daily Energy of 1 MW	Power losses, EV charging costs Voltage fluctuations, battery degradation	GA-PSO
[15]	Max 80 kW	LPSP, LCOE, CFOE and socio-political,	NWCMO+ PSO
This study	Max allowed by different categories of EVs	NPC, Pollutant Emission	Linear scalarization +GA

This work aims to optimize the configuration of a UFCS by minimizing its NPV and environmental impact. The components considered inside the station are the connection with the utility grid, a PV, and a BESS. The decision variables of this study are the PV module number as well as the battery number. The bi-objective optimization problem is then reduced to a single-objective one by employing the linear scalarization method, and finally, the overall objective function is solved through GA.

The main contributions of this paper are as follows:

1) The power demand of a UFCS is computed taking into account all the stochastic variables of EVs, such as the arrival time to the station, the initial State-of-Charge (SoC), the different charging characteristics of EVs belonging to different categories (e-cars, heavy-duty electric vehicles, e-motorbikes).
2) A bi-objective optimization model is used to determine the optimal size of on-site PV panels and BESS.
3) A case study and a sensitivity analysis are performed to demonstrate the impacts of various parameters on the optimal solution.

The rest of this paper is as follows. In Section II, the load demand of the UFCS is introduced. Then, the overall system of the station along with the model of each of its components is displayed in Section III. In Section IV, the objective functions and the optimization method are described. The case study is presented in Section V, along with the results and the sensitivity analysis on the UFC station. Finally, conclusions are given in Section VI.

II. LOAD POWER DEMAND

A necessary step to perform the sizing optimization of the charging station is to estimate the daily electric power

required by the EVs which connect to the station. Therefore, given the importance of a priori knowledge of the daily load profiles, in literature can be found many studies that try to assess the effects of EVs charging on the grid. Most of them focus on residential charging [16]–[18]. For instance, in [16], the authors compare time-series techniques and machine learning methods used to forecast the growth in building power consumption caused by the rising of EV chargers. According to the results, the machine learning techniques have the advantage of requiring few initial assumptions, but they do not always show good predictive results. In this study, the authors start from the assumption that a sufficient complete database with historical data was available, which is not always the case, particularly for such a new technology. Indeed in [19], the author employs a bottom-up approach to assess the EVs charging impact on residential consumption without relying on historical data. Many other studies in literature focus on the impact of EVs charging in commercial [20] and office buildings [21]. Instead, little research can be found on the impact of ultra-fast charging with power rates higher than 50 kW per charger. In fact, for this particular type of infrastructure, historical data are not available, and this could become a critical concern because an improper estimation of the load profile can easily lead to underestimate or overestimate their impact on network planning and operation. Since historical input data are not available, the charging station profiles can be mainly computed through two types of approaches: probabilistic and deterministic. In [22] the authors estimate the impact of a fast-charging station with a power output of 250 kW for each charger. They compare the two above-mentioned approaches and according to the results the probabilistic one seems to show a more realistic consumption. However, in the assessment, the authors assume that all the connected vehicles charge at the maximum power of 250 kW for the whole duration of the charging process (from 10% up to 80% of SoC). In [23] a UFC station with charging ports of 150 kW each is considered and in this case the authors take into account also the charge acceptance curves of the vehicles assumed to be charged at the station, however, they investigate just three models of Nissan Leaf as EVs fleet. In [24], a probabilistic approach is chosen a priori and the results present the daily power demand profiles of a FCS to changes in different quantities such as the distances covered by the commuters, the availability of slow charge at home and the number of chargers in the station. Finally, in [25] the hourly power demand of an ultra-fast charging station installed along a highway based on a probabilistic approach is carried out. In this reference, the charging capabilities of the different electric cars models is not considered and moreover, only cars are assumed to stop at the station All the listed studies agree that a probabilistic approach brings sounder and more realistic results, therefore this method is used to find the EV arrival time and SoC in this study. In addition, in the EVs load demand here simulated, different categories of EVs will be investigated with their relative charging profiles. The assumptions made to compute the load demand of the station are discussed below.

1) As mentioned in the previous section, in this study, a UFCS is considered. This type of charging system is necessary to serve EV when medium- or long-distance travels are concerned. Consequently, the typical installation of UFCS is along motorways.
2) The UFCS aims to fill the EV batteries as fast as possible, and hence, the maximum allowable charging power in this study is not limited by the infrastructure but from the EVs batteries performances.
3) The number of charging ports in the station, the maximum waiting time the drivers are willing to wait, the EV penetration level, and the EV typologies division are inputs variables; so that, the optimization procedure in this study can be easily adapted to different scenarios.
4) The charging power strongly depends on the battery SoC. Indeed, as the battery approaches SoC around 60-70%, the charging rate starts to drop quickly [26], and the UFCS becomes quite useless. For this reason, it is assumed in this work that all the EV will charge their batteries up to 90%, apart from the heavy-duty vehicles that, given their large battery capacity, are assumed to charge up to 100%.

Finally, the flowchart of the process followed to compute the UFCS load profile is reported in FIG. 1.

A. ELECTRIC VEHICLES ARRIVAL TIME

The arrival time distribution of EVs at a UFCS placed along a highway can be assumed equivalent to the arrival time distribution of Internal Combustion Engine (ICE) vehicles at a petrol service station [25], [27]. Indeed, if the arrival time distribution of a charging station in an urban context cannot be assumed equal to that of the petrol station, since the refueling durations are different, UFCSs along highways tend to simulate the service as similar as possible of the actual fueling service area.

Therefore, to simulate the probability density function of EVs' arrival times at the station, the actual traffic flow data provided by the Italian National Road Authority was used [28]. These data refer to hourly traffic flows of typical working and weekend days in a service area with a petrol station installed along a highway in the North of Italy. The data were divided for weekdays and weekend days and the corresponding probability functions are reported in FIG. 2. Two peaks can be recognized, the morning peak (08.00 am–10.00 am) and the evening peak (16.00–20.00). This pattern can be easily understood because these are the times when most commuters and businesspeople depart and return home to/from their work destination.

B. ELECTRIC VEHICLES ARRIVAL STATE OF CHARGE

The SoC of the EV arriving at the station is modeled by the Weibull probability density function [29] described by (1), where a and b are the scale and shape factor, respectively,

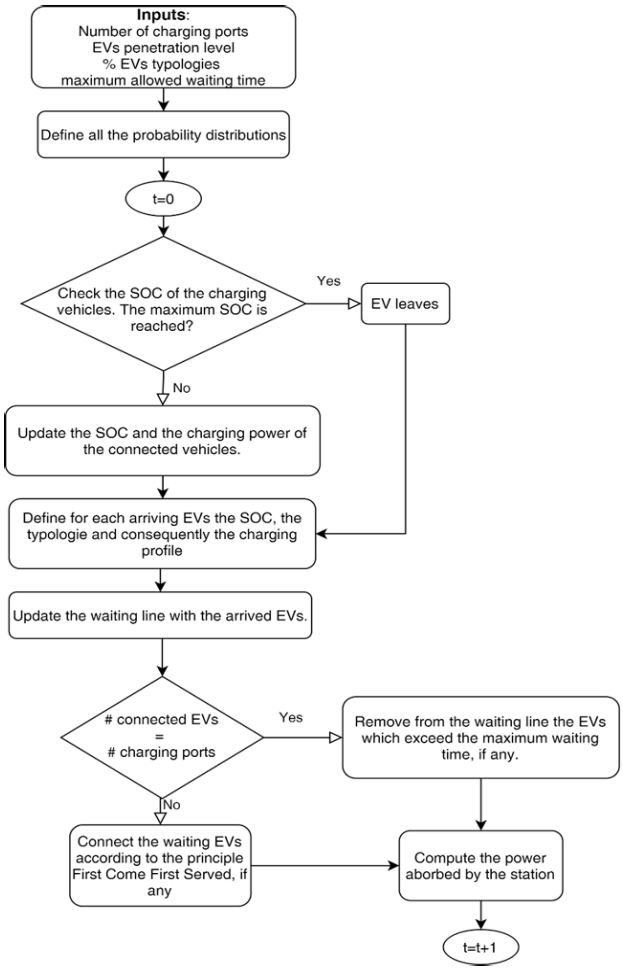

FIGURE 1. Flowchart of the steps to compute EVs demand.

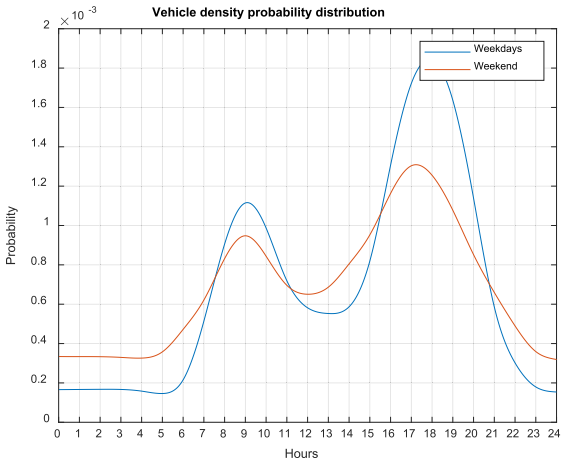

FIGURE 2. Probability distribution of the EV arriving time to the station.

which in this study were set at 2.4 and 2.5.

$$f\,(SOC|a,b) = \frac{b}{a}\cdot\left(\frac{SOC}{a}\right)^{b-1}\cdot e^{-(SOC/a)^b} \qquad (1)$$

The distribution is shown in FIG. 3, it has a peak around SOC equal to 20%, indeed according to [20] and [30] the EVs users are more likely to charge their EVs when their SOC is low and in the range of 15%-25%, instead for lower values EV drivers would worry about running out of electricity on the middle of the way. Then, the probability decreases almost equally on both sides; for SOCs higher than 60%, the probability of stopping at the station to charge is almost null.

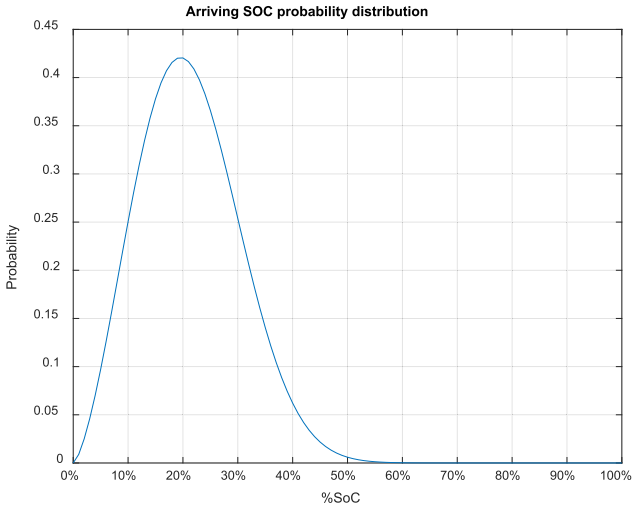

FIGURE 3. Probability distribution of the SoC of EV arriving to the station.

C. ELECTRIC VEHICLES CHARGING PROFILES

The charging time of an EV does not depend only on the output power of the charger, but it is determined also by the vehicle charging capability, which in turn depends on multiple factors, among which the most significant are the battery temperature and the maximum rate of charge allowed by the manufacturer (usually about 2C). This latter in turn strongly depends on the capacity of the battery.

In the considered EV fleet, the following categories are included: an electric moto, three types of electric cars having different batteries capacity (small, medium, large), and an electric heavy-duty vehicle (i.e. e-bus, e-truck). Their charging profiles, shown in FIG. 4 can be found in [31] and [32].

III. MODEL OF SYSTEM COMPONENTS

In the considered UFCS, the energy required by the connected EV can be provided by the utility grid, by the installed PV panels, and by the BESS. It is assumed that the energy cannot be sold back to the grid. This hypothesis is justified from the fact that in this type of charging system the EV needs to be charged as quickly as possible, and hence they are not interested in participating in the vehicle-to-grid (V2G) technology. One of the main disadvantages of this type of charging station is that it requires a very high initial investment cost and further increasing the cost to provide V2G is not the case. Therefore, in this study, if an extra amount of solar energy is generated only the BESS can be used to store it.

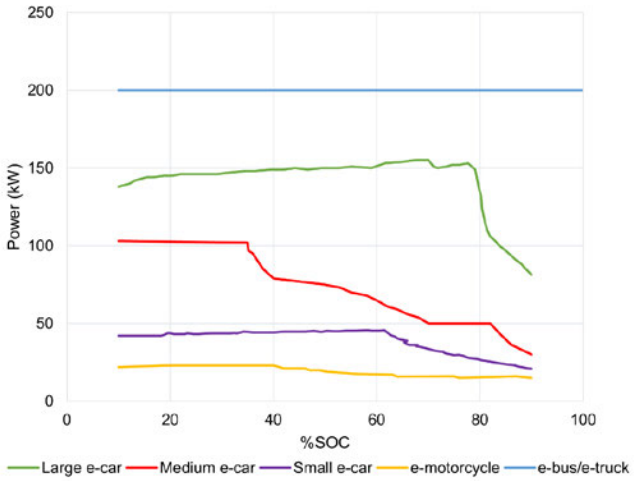

FIGURE 4. Charging profiles of the considered EV typologies.

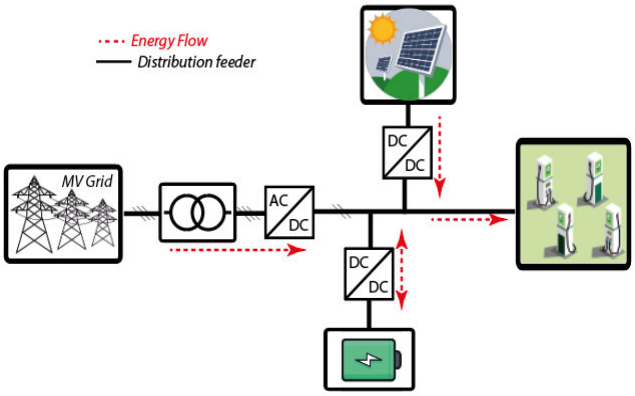

FIGURE 5. Schematic model of the station.

In Fig. 5 the schematic model of the system is presented. It consists of PV panels, BESS, medium voltage power grid, ultra-fast chargers, and EV.

1) Given the high power required by the UFCS, the connection to the utility grid cannot take place directly from the low voltage but it must be connected to the primary medium voltage (MV) distribution.
2) In this case, the grid only supplies electricity to the station when the energy generated from the PV system and stored in the BESS cannot satisfy the EVs demand. The system purchases electrical energy from the grid under real-time electricity prices.
3) A DC bus architecture is chosen for the considered station since it allows easier integration of RES and ESS.
4) The BESS is connected to the common DC bus through a bidirectional DC/DC power converter.
5) The PV panels are connected to the common DC bus through a unidirectional DC/DC power converter.
6) The EVs are the main load of the station. They can only absorb power from the system.

A. PHOTOVOLTAIC PANELS

A PV system converts the sunlight into DC electricity. Therefore, photovoltaic system, with their free-emission energy, is considered one of the best alternatives for replacing traditional fossil fuel-based power resources soon. Moreover, it has become an essential component in the construction process of smart cities and smart grids, indeed, several projects around the world have been studying charging electric cars with installed solar panels in parking lots. Nevertheless, the output power of a PV system is not controllable but it depends on many factors; the most relevant ones are meteorological conditions, temperature, solar irradiance, and PV panels area [33], [34].

The PV panel output power in the time instant t is reported in (2).

$$P^*_{PV}(t) = P^r_{st} \cdot \frac{G(t)}{G_{st}} \cdot \delta \cdot [1 - \alpha\,(T_c(t) - T_{st})] \tag{2}$$

where P^r_{st} is the rated power of the PV module; G is the global solar radiation incident on the module measured in kW/m^2; G_{st} is the incident radiation at standard test conditions (i.e. 1 kW/m^2); δ is the derating factor in (%); α is the temperature coefficient (°C), which ranges from 0.004 to 0.006 for silicon cells [35]; $T_c(t)$ is the cell temperature at t of the PV array (°C) and T_{st} is the cell temperature at standard conditions (25°C).

Since the optimization aims to determine the number of PV panels to be installed, the output power produced by N_{pv} panels is expressed in (3).

$$P_{PV}(t) = N_{PV} P^*_{PV}(t) \tag{3}$$

Finally, in this study, the approximation in (4) is considered in the model of the PV system. For low-temperature conditions, the effect of temperature can be neglected, and hence α can be set at zero.

$$P_{PV}(t) = N_{PV} \cdot P^r_{st} \cdot \frac{G(t)}{G_{st}} \cdot \delta \tag{4}$$

The efficiency of the DC/DC converters has been neglected in this study because it is assumed that the power losses have a low impact on the total energy flow and costs.

B. BATTERY ENERGY STORAGE SYSTEM

Battery energy storage systems are devices that enable energy from RES, like solar, wind, and hydro to be stored and then released when customers need it the most. Coupled with a UFCS, BESS can reduce the operational costs of the charging infrastructure by supplying the EVs during peak load times. Moreover, the storage system can also lead to lower system (transformer and feeder) up-gradation costs by purchasing energy from the national grid during off-peak intervals [36]. Different technology can be used for battery storage: Lead-acid, Nickel-cadmium, Nickel-metal hydride, and Li-ion batteries. A complete comparison of these types of batteries can be found in [37].

The proposed optimization aims to find the optimal capacity of the BESS to be integrated into the charging station. The main aim of this component is to perform the balance between the generation sources and loads. The mathematical model used for the BESS is shown in (5)-(7) [12].

The charging process is expressed through (5):

$$E_{BESS}(t) = E_{BESS}(t-1)(1-\beta) + (P^{ch}_{BESS}(t) \cdot \eta^{ch}_{BESS} \cdot \Delta t) \tag{5}$$

The discharging process is shown in (6):

$$E_{BESS}(t) = E_{BESS}(t-1)(1-\beta) + (P^{dis}_{BESS}(t) \cdot \eta^{dis}_{BESS} \cdot \Delta t) \tag{6}$$

Therefore, the overall equation for this component becomes:

$$E_{BESS}(t) = E_{BESS}(t-1)(1-\sigma) + [P^{ch}_{BESS}(t) \cdot \eta^{ch}_{BESS} \cdot \lambda_1(t) - P^{dis}_{BESS}(t) \cdot \eta^{dis}_{BESS} \cdot \lambda_2(t)] \cdot \Delta t \tag{7}$$

where $E_{BESS}(t)$ is the energy of the battery at time t; $E_{BESS}(t-1)$ is the energy at time $t-1$; σ is the battery self-discharge rate; P^{ch}_{bess} is the charging power at time t; η^{ch}_{BESS} and η^{dis}_{BESS} are the charging and discharging efficiency, respectively; and Δt is the considered time interval.

The variables $\lambda_1(t)$ and $\lambda_2(t)$ define the operation of the BESS according to the following rules:

$$\lambda_1(t) = \begin{cases} 1 \rightarrow \textit{the battery is charging} \\ 0 \rightarrow \textit{the battery is not charging} \end{cases} \tag{8}$$

$$\lambda_2(t) = \begin{cases} 1 \rightarrow \textit{the battery is discharging} \\ 0 \rightarrow \textit{the battery is not discharging} \end{cases} \tag{9}$$

Since the battery cannot discharge and charge at the same time the constraint in (10) comes naturally:

$$\lambda_1(t) + \lambda_2(t) = 1 \tag{10}$$

The other constraints related to this component are expressed from (11) to (13).

$$P^{dis}_{BESS}(t) < P^{dis}_{max} \tag{11}$$

$$P^{ch}_{BESS}(t) < P^{ch}_{max} \tag{12}$$

$$E^{min}_{BESS} \leq E_{BESS}(t) \leq E^{max}_{BESS} \tag{13}$$

The first two constraints imply the fact that the charging and discharging power cannot exceed the rated values of the battery declared by the manufacturer. Instead, the last restriction specifies that the SoC of the battery cannot outstrip the minimum and maximum limits.

The minimum limit E^{min}_{BESS} is computed through (14).

$$E^{min}_{BESS} = (1 - DOD)E^{max}_{BESS} \tag{14}$$

where DOD is the battery's depth-of-discharge, which refers to how much energy can be taken out of the battery on a given cycle, and it is expressed as a percentage of the total capacity. In the simplified model of this component aspects such as battery degradation [38], [39] and safety constraint like over-temperature [40] have been neglected for the sake of simplicity, however their impact can be introduced in future improvements of this work.

IV. OPTIMIZATION FORMULATION

A. OBJECTIVE FUNCTION

As previously mentioned, a multi-objective optimization is performed in this study. The objective function to be minimized is hence composed of an economic and an environmental objective. The two functions are joint in the final one through the weighted sum method.

1) ECONOMIC FUNCTION

The economic optimization of the PV panels and BESS size is performed concerning the Net Present Cost (NPC) or also known as Life Cycle Cost (LCC). The NPC includes the annual cost of each *k-th* component in the station AC_k and the annual cost of purchasing electric energy from the national grid C_{grid}. In particular, the k components are the PV sources and the BESS, since the cost of the charging infrastructure is not considered. Therefore, the formula to compute NPC is reported in (15):

$$NPC = \sum_{k=1}^{m} AC_k \cdot N_k + \frac{C_{grid}}{CRF} \tag{15}$$

where N_k is the number of units of the *k-th* component; and CRF is the capital recovery factor, whose formula is shown in (16), which depends on the interest rate i and on the system lifetime y.

$$CRF(i, y) = \frac{i \cdot (1+i)^y}{(1+i)^y - 1} \tag{16}$$

The total cost in one year AC_k of each component includes the annualized capital cost AIC_k, the annual operation and maintenance cost $AO\&M_k$, the annual replacement cost ARC_k and residual value RV_k. A full explanation of how to compute the annualized costs is reported in [41] and [42]. In this model, the lifespan of the charging station and the PV panels is assumed the same and hence the residual value and the replacement costs of this component are nil. Also, for the battery, the lifespan is considered equal to that of the PV systems and the project, however, to achieve this time a replacement in the middle of the project lifespan is necessary. Therefore, the ESS residual value will be nil too. The final formula to compute the annual cost of each considered component is given in (17) and (18).

$$AC_{PV} = AIC_{PV} + AO\&M_{PV} \tag{17}$$

$$AC_{BESS} = AIC_{BESS} + ARC_{BESS} + AO\&M_{BESS} \tag{18}$$

Finally, the annual electricity cost is computed in (19):

$$C_{grid} = \sum_{t=1}^{T} (P_{grid}(t) \cdot E_{pr}(t)) \tag{19}$$

where E_{pr} is the electricity price at time t; and $P_{grid}(t)$ is expressed in (21).

2) ENVIRONMENTAL FUNCTION

The introduction of renewable sources will bring a positive effect on the global emissions of the station, as a matter of fact, the EVs batteries will be supplied by pollution-free energy when the solar one will be available. Consequently, in the overall statement, pollutant emissions primarily occur because of the amount of electricity supplied by the national grid.

The second objective, shown in (20) aims to minimize the emissions of the main following atmospheric pollutant: Nitrogen oxides (NO_x), Sulphur dioxide (SO_2), and Carbon dioxide (CO_2).

$$E_{poll} = \sum_{t=1}^{T} \left(E_{CO_2}(t) + E_{SO_2}(t) + E_{NO_X}(t)\right) = \begin{cases} 0 & \rightarrow P_{grid}(t) = 0 \\ P_{grid}(t)\left(e_{CO_2} + e_{SO_2} + e_{NO_x}\right) & \rightarrow P_{grid}(t) \neq 0 \end{cases} \tag{20}$$

where E_{poll} is the total pollutant emission; $E_{CO_2}(t)$, $E_{SO_2}(t)$, and $E_{NO_X}(t)$ refer to the CO_2, SO_2, and NO_x emission at time t, respectively; and finally, e_{CO_2}, e_{SO_2}, and e_{NO_x} are the emission factors of CO_2, SO_2, and NO_x, respectively, which are set depending on the selected energy mix.

3) CONSTRAINTS

The overall objective function must be minimized satisfying the following constraints:

1) Equality constraints: the system must meet the energy balance, which means that the power required in each instant of time t by the charging load has to be equal to the sum of the power provided by the PV panels, the BESS, and the grid. This constraint is given by (21), where η_{ch} is the efficiency of the charging system of the EV.

$$\frac{P_{EV}(t)}{\eta_{ch}} - P_{PV}(t) + P^{ch}_{BESS}(t) \cdot \eta^{ch}_{BESS} \cdot \lambda_1(t) + -\frac{P^{dis}_{BESS}(t)}{\eta^{dis}_{BESS}} \cdot \lambda_2(t) = P_{grid}(t) \tag{21}$$

This equality constraint includes also the limit coming from the fact that the BESS cannot be discharged and charged at the same time, which is expressed in (10). Ultimately, the two decision variables N_{PV} and N_{BESS} are chosen to be positive integer numbers.

2) Inequality constraints: this type of constraint includes the limits related to the BESS component which are reported from (11) to (13) and, in addition, the limit shown in (22), which states that the station can only purchase electricity from the gird.

$$P_{grid}(t) \geq 0 \tag{22}$$

B. OPTIMIZATION METHOD

The bi-objective optimization model is solved through the weighted sum method, also known as the linear scalarization method. As shown in (23), in this method, a weight factor is assigned to each objective in the problem, and then, the weighted sum is optimized.

$$min\, f(x) = min \sum_{i=1}^{n} w_i \cdot f_i(x) \tag{23}$$

where f is the overall objective function; and w_i are the weights of the n objectives which must satisfy (24).

$$\sum_{i=1}^{n} w_i = 1 \tag{24}$$

In other words, with this approach, the multi-objective problem is converted into a single-objective optimization problem, so that the optimal solutions of the single-objective problem are Pareto optimal solutions to the multi-objective one. Therefore, considering a bi-objective problem, (23) becomes:

$$\min f(x) = \min\left[w_1 \cdot f_1(x) + w_2 \cdot f_2(x)\right] \tag{25}$$

$$w_2 = 1 - w_1 \tag{26}$$

where w_1 is chosen in the range [0-1]; and w_2 is computed according to (26).

The objective functions considered in the multi-objective optimization problem, however, are usually measured in different units, and hence, can have significantly different orders of magnitude. This can be a problem for depicting the Pareto optimal set since the aggregated function can be dominated by one or more objectives within it. To overcome this issue, a function transformation can be applied to normalize the different objective functions [43].

Different functions transformations have been studied in literature and a complete review can be found in [44]. Among these, the upper-lower-bound approach is the most effective and robust method, and thus, it is chosen for this study.

According to this method, the transformed function is defined as:

$$f_i^{transf} = \frac{f_i - f_i^0}{f_i^{max} - f_i^0} \tag{27}$$

where f_i^0 is the minimum feasible value of the *i-th* objective function, obtained by minimizing $f_i(x)$ without taking into account the other objectives. Instead, f_i^{max} is defined in (28).

$$f_i^{max} = \max_{k \neq 0} f_i(x_k) \tag{28}$$

where x_k is the point that minimizes the *k-th* objective.

To put it simply, f_i^{max} is the maximum value of $f_i(x)$ obtained for solutions that minimize all the other $f_k(x)$ functions with $k \neq i$. In the studied bi-objective optimization, f_1^{max} is obtained by minimizing $f_2(x)$ by setting $w_2 = 1$ and $w_1 = 0$. Once obtained the x value which minimizes f_2, this

is substituted in f_1, and f_1^{max} is obtained. The same procedure is applied to find f_2^{max}.

The function transformation expressed in (27) is applied to the bi-objective function in (25) and the ultimate single-objective function to be optimized is expressed in (29):

$$f_{final}(x) = w_1 \cdot \frac{f_1(x) - f_1^0}{f_1^{max} - f_1^0} + w_2 \cdot \frac{f_2(x) - f_2^0}{f_2^{max} - f_2^0} \quad (29)$$

where x indicate the set of decision variable, which in this case are the number of PV panels (N_{PV}) and batteries (N_{BESS}) to be installed; f_1 is the NPC of the station expressed in (15); and f_2 expresses the pollutant emissions E_{poll} computed in (20).

One of the most used heuristic methods to solve single-objective optimization problems characterized by many stochastic variables is the GA [45], [46]. The fundamental law of GA is to seek optimal solutions using an analogy with the theory of evolution [47]. The basic GA steps are shown in FIG. 6. The MATLAB software, precisely its optimization toolbox in which GA is already embedded, is used to run the proposed optimization.

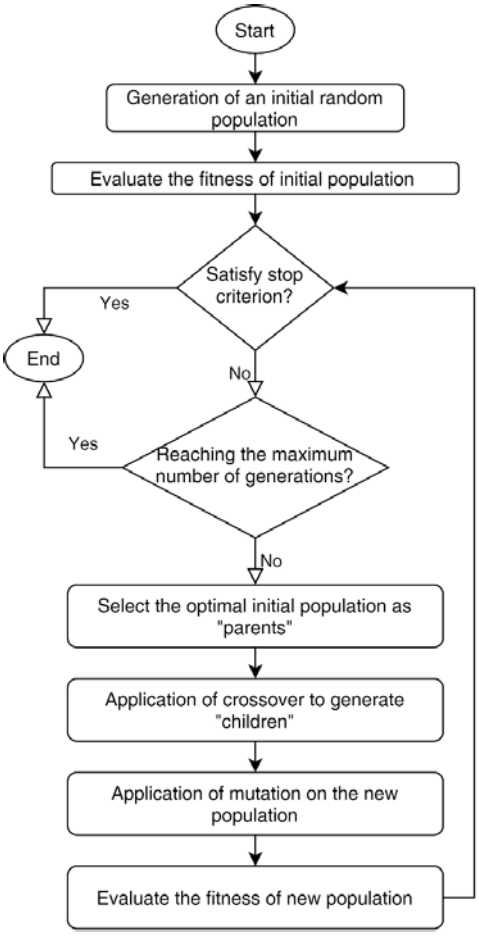

FIGURE 6. GA flowchart.

V. RESULTS AND DISCUSSION

A. CASE STUDY

In this section, all the input parameters used for the installation case along the Italian highway are defined.

1) LOAD DEMAND

In the proposed UFCS, 6 charging ports are considered. The rated power of each pile is assumed to be 200 kW. Therefore, by comparing this value with the charging profiles in FIG. 4. it can be noticed that the limit charging power is imposed by the Battery Management System (BMS) of the EV battery and not by the infrastructure.

The EVs penetration level is established at 30%, a value which is expected to be reached in 2030 in Europe [48]. With such a penetration level, at the considered station, 100 EVs are expected to arrive on a weekday and 95 on a weekend day. The EVs arriving at the station are divided according to the category percentages reported in FIG. 7 [49]. The share of different categories has been carefully selected attempting to reflect reality and to present a foreseeable future scenario. It has been differentiated not only on the type of vehicle but also on the day.

As can be seen from FIG. 7, most of the fleet (90%-95%) is composed of electric cars car since this is the vehicle that has the highest penetration share on the market in Italy [50]. For the electric motorbikes, we have considered a share of 2% because even if some models of e-motorbike (just referring to those having power higher than 11kW, otherwise they cannot enter Italian highways) have been recently introduced on the market, however, their penetration level is still low [51]. Finally, regarding the low share of electric trucks, it is

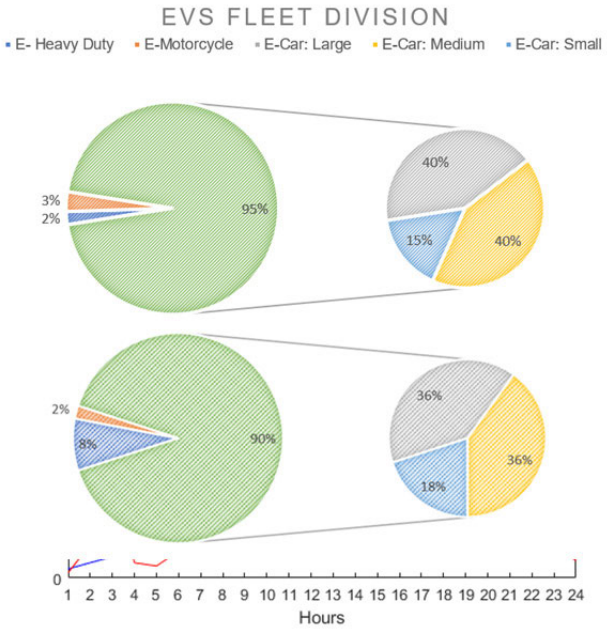

FIGURE 7. Fleet division by EVs categories.

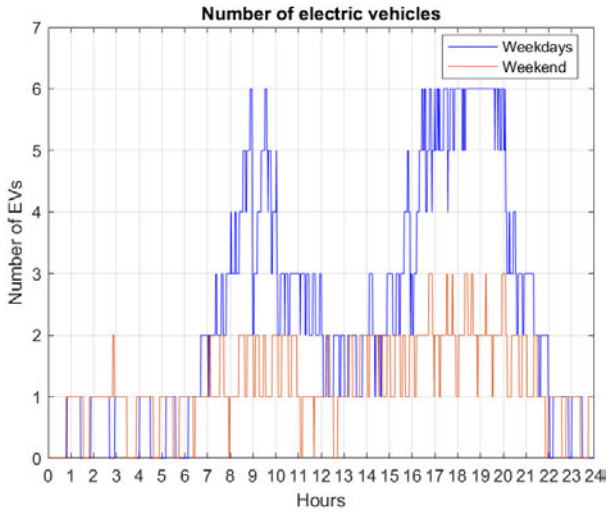

FIGURE 8. Estimated number of EVs connected to the station.

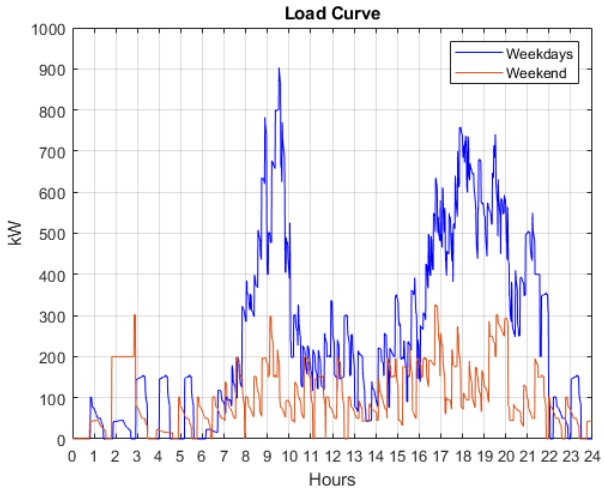

FIGURE 9. Estimated EVs daily demand.

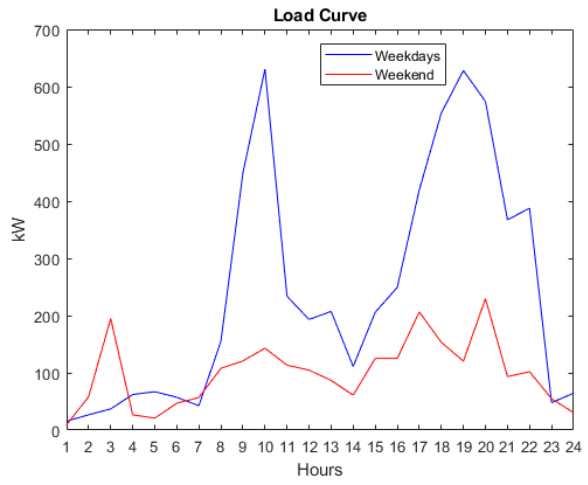

FIGURE 10. Estimated EVs daily demand with Δt of 1 hour.

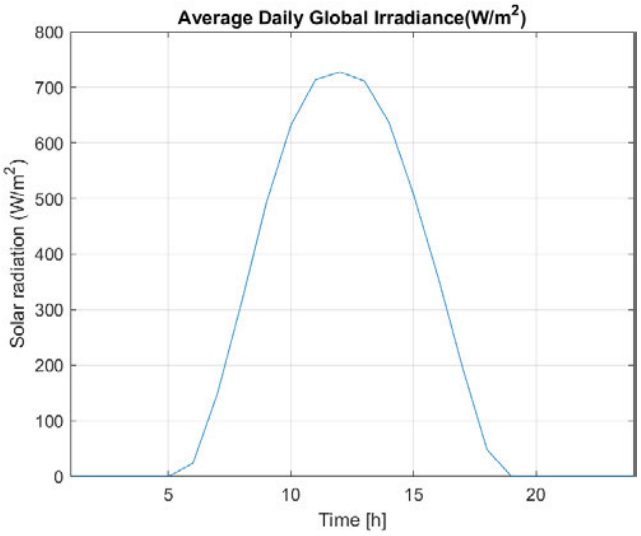

FIGURE 11. Average daily global irradiance.

reasonable to suppose that battery-electric mobility will not strongly affect this category. Indeed, hydrogen can be a more suitable solution for heavy road transport [52], [53]. On the weekend the share of this category is further decreasing because of the presence of a Sunday traffic ban for heavy-duty trucks [54].

Finally, the number of EVs connected to the station throughout the day is presented in FIG. 8 and the maximum waiting time the EV drivers are willing to wait has been set at 15 minutes.

By inserting all the above-discussed values as input and following the procedure described in Section II, the EVs demand is computed and reported in FIG. 9. However, since in the analysis a one-hour time interval length is chosen, the EVs demand is approximated as in FIG. 10.

2) PHOTOVOLTAIC PANELS AND BATTERY ENERGY STORAGE SYSTEM

The information related to solar radiation is collected from local meteorological data. The considered average daily global irradiance in a year $G(t)$ of the PV panel is shown in FIG. 11. All the input parameters required in the models of the ESS, and the PV panel are defined in Table 2 and Table 3, respectively.

3) ELECTRICITY PRICE AND GRID EMISSIONS

The electricity exchange with the utility grid is based on interval electricity tariffs, which are reported in Table 4. The interest rate is set at 6%.

To compute the environmental impact of the station, the following emission factors, computed according to the Italian Energy mix [55], are used: 250, 0.198, and 0.058 g/kWh for e_{CO_2}, e_{SO_2}, and e_{NO_x}, respectively.

Finally, the lower and upper limits for the number of PV panels are set at 1 and 200, respectively; and for the BESS to 1 and 50.

TABLE 2. Parameters of the BESS.

Parameter	Value	Unit
Capacity	50	kWh
Rated power	25	kW
DOD	80	%
Charging efficiency	96	%
Discharging efficiency	92	%
Self-discharging rate	0.002	-
Initial cost	17000	€
M&O cost	120	€/year
Replacement cost	15000	€
lifetime	20	year

TABLE 3. Parameters of the PV panel.

Parameter	Value	unit
Rated Power	6.02	kW
Modules	28x0.215	kW
derating factor	85	%
Initial cost	9000	€
M&O cost	100	€/year
lifetime	20	year

TABLE 4. Energy prices.

Time-of-Use	weekday	Saturday	Sunday	Price [€/kWh]
F1 (peak)	08-19	-	-	0.18
F2 (mid-peak)	07-08 19-23	07-23	-	0.12
F3 (off-peak)	23-07	23-07	0-24	0.08

TABLE 5. Costs and emissions in different cases.

Parameter	Value	N_{BESS}	N_{PV}
Min. Emission	$2.25 \cdot 10^8$ g/year	1	200
Min. NPC	$1.46 \cdot 10^6$ €	25	90
Max. Emission	$4.39 \cdot 10^8$ g/year	0	0
Max. NPC	$3.01 \cdot 10^6$ €	0	0

B. RESULTS

1) SCENARIO A: THE BATTERY CAN BE RECHARGED BY THE GRID

In the analyzed scenario, the energy management system of the station can be summarized with the following steps:

1) If the production of solar energy exceeds or matches the EV demand, then the EV batteries will be supplied only from the PV panels, and the extra-solar energy, if present, will be stored in the BESS, if possible, and otherwise will be wasted.
2) In the case that the load demand is higher than the power produced by the PV panels and the grid energy price at that moment is in the F3 tariff, the extra amount of required power is supplied by the grid. In this scenario also the BESS is charged by the grid.
3) Finally, if the solar energy is not enough but the energy price is in F1 or F2, then the extra amount of power will be supplied by the ESS and by the utility grid when necessary.

To demonstrate the advantages coming from the installation of the PV panels and ESS, Table 5 illustrates the life-cycle costs and the emissions of the UFCS with and without the installation of these components. It is displayed that considerable cost and emissions savings can be reached by integrating the PV and ESS in the station design. For instance, with these components, the minimum achievable NPC of the charging station, reached with the installation of about 540 kW of PV panels and about 1.25 MWh of energy storage capacity, could be reduced by 55% with respect to the case without any additional components. Similarly, the pollutant emissions of the overall station in one year of operation can be halved to $2.25\ 10^5$ kg per year.

The weight factors cannot be chosen a priori since they reflect the preferences of the possible different station owners in the decision-making process. For instance, if the NPC objective has a higher weight, it means that the owner is more interested in obtaining economic benefits from the system. On the contrary, if the emission objective has a higher weight factor it implies that the investor is more in pursuit of environmental benefits.

The system configuration and objective function values under the influence of different weight factors are illustrated in FIG. 12 a) and b), respectively. It can be seen that the number of batteries increases while the number of PV decreases, with the increase of the weight of the economic objective (objective 1). The weight factors variation directly leads to a change in the value of the objective functions. As displayed in FIG. 12 b), as w1 rises gradually, the value of NPC drops, while the emissions become larger. However, for values of w1 up to 0.3, there is no change because the number of PV panels coming from the optimization is equal to the set upper limit of 200 units as well as the number of batteries is at the minimum of 1 unit.

Supposing that the weight of each objective function is 0.5, the output power, per hour on a weekday, of the PV system and the grid as well as the power required from the load and the ESS SoC are illustrated in FIG. 13. It can be seen that the BESS discharges completely between 18-22 h, and with a small depth between 8-11 h, when the electricity prices are in the highest range. However, in the middle of the day, even if the electricity prices are high, the ESS has recharged at 100% thanks to the extra solar energy produced by the PV panels.

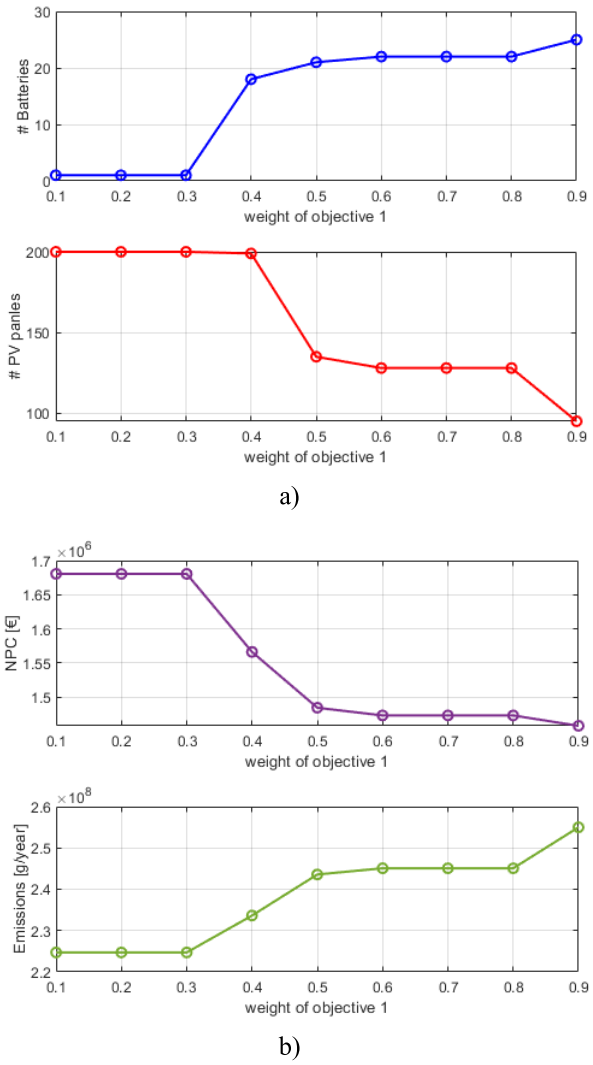

FIGURE 12. Variation for different weight factors of a) decision variables, b) objective function values.

2) SCENARIO B: THE BATTERY IS NOT RECHARGED BY THE GRID

In this scenario, the energy management system is the same as the previous one, except for the fact that the BESS is not recharged during the F3 tariff. Therefore, this implies the fact that the BESS is never charged by the grid, but it can be filled only with surplus solar energy coming from the installed PV system. According to results obtained (with the weight factors set at 0.5), the best configuration, in this case, would require the installation of 74 battery units of 50-kWh and the presence of 197 6-kW solar panels. As expected, the number of required PV units increases near the maximum upper limit of 200 units since in this scenario the solar energy must satisfy both the EVs and the battery needs.

FIG. 14 a) and b) show the SOC of the BESS system throughout a weekday and a weekend day for both Scenario A and B, respectively. As can be seen, in Scenario B since the battery cannot be recharged during the lowest electricity rate intervals with the energy bought from the national

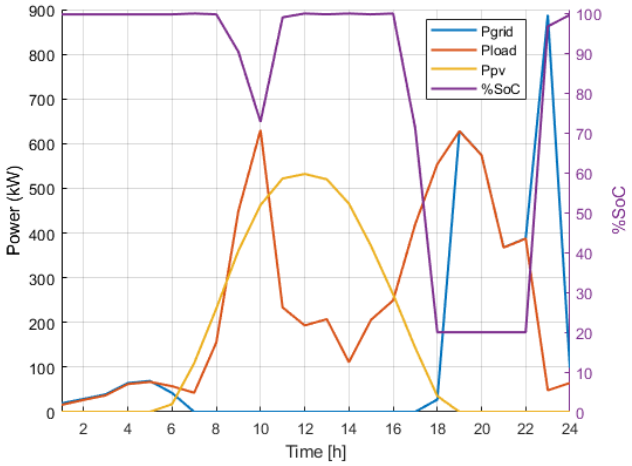

FIGURE 13. PV, load and grid power, and SoC of ESS per hour in one weekday.

electric grid, it ends its operation at 23 h fully discharged since it provides energy to the EVs during the peak demand interval which goes from 17-23 h and it starts its charging process with the surplus solar energy in the early morning at 7 h. Instead in Scenario A, the battery contributes both in the peak load intervals with a not deep discharge between 9 h up to 12 h and with a complete discharge in the afternoon peak from 17 h to 19 h. Then it is completely recharged with the energy purchased from the grid with the lowest tariff starting from 23 h.

Nevertheless, the NPC of the station in Scenario B results to be about 1.64 M€which means 10.5% more than Scenario A. The produced emissions of CO_2 result $2.6\ 10^8$ g/year and hence higher by about 7% than Scenario A. Therefore, we can conclude that purchasing energy from the grid during the lowest peak electricity prices to charge the BESS is more convenient both in environmental and economic terms.

C. SENSITIVITY ANALYSIS

In order to verify the effectiveness of the problem and to identify which are the factors that influence the most the optimal design, in this section a sensitivity analysis is carried out.

1) BATTERY PRICES

The prices of lithium-ion batteries enormously vary depending on the technology. However the cost of all the technologies is declining every year, and a reduction of up to 60% of the actual cost can be expected in 2030 [56]. In FIG. 15, the trends of the amount of PV panels and batteries to be installed in the station are reported for battery prices varying in the range of 200-1000 €/kWh. The weight factors are both set at 0.5.

As can be seen, the battery cost does not strongly affect the number of batteries for a price variation up to 800 €/kWh. However, in the range 800-900 €/kWh, a sudden and

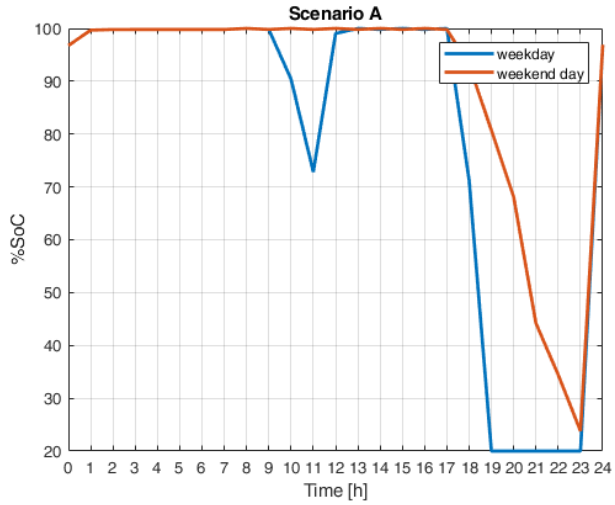

a)

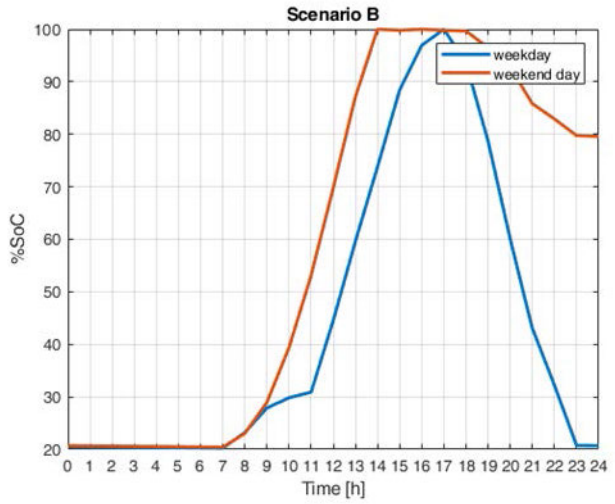

b)

FIGURE 14. SoC of the BESS throughout the day in: (a) Scenario A and (b) Scenario B.

significant decrease occurs, and the optimal number of batteries passes from 21 to 8 units.

2) ELECTRIC VEHICLES CHARACTERISTICS AND PENETRATION LEVEL

The battery is the most challenging component inside the EV because of its high cost and reduced driving range. The rapid fall of prices and the continuous and quick technological improvements of this component will positively affect the EV market [57]. Indeed, lower battery prices will automatically result in larger battery capacities and an increase in the sells due to lower EV prices. Therefore, considering this plausible future scenario, the decision variables are reported in Table 6 for different load scenarios. Only electric cars are assumed to be charged in the station.

As expected, if the e-cars penetration level increases the optimal design expects more ESS capacity and PV modules to be installed. Precisely if the penetration level triplicates, the

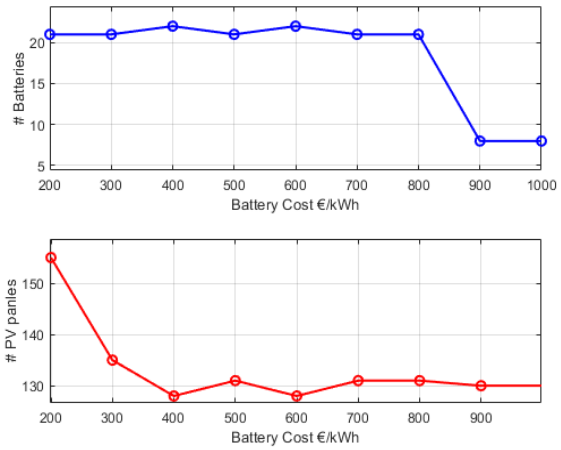

FIGURE 15. Decision variables for battery price variations.

TABLE 6. Decision variables for different load demands.

#e-car weekday and weekend	Small, Medium Large %	N_{bess}	N_{pv}
50, 30	L=30% M=40% S=30%	11	84
50, 30	L=60% M=40% S=0%	11	108
100, 60	L=30% M=40% S=30%	21	126
100, 60	L=60% M=40% S=0%	24	141
150,90	L=30% M=40% S=30%	29	200
150, 90	L=60% M=40% S=0%	31	200

number of ESS units almost triplicates too, and the amount of PV panels reaches the maximum limit of 200 units.

3) ELECTRICITY PRICES

The influence of the electricity prices on the optimal configuration is here analyzed. The four simulated scenarios are depicted in Table 7. The time division of Table 4 is still valid. Moreover, as it can be seen, the difference among the prices is kept unchanged, which means that the prices of F2 are 50% higher than those of F3, and the prices in F1 are 50% higher than those in F2.

The results are shown in FIG. 16. In scenarios from 2 to 4, an increase in the prices of the electricity purchased from the grid corresponds to an increase in the number of PV panels to be installed as well as to a slight decrease in the number of

TABLE 7. Electricity prices scenarios.

Scenario	F3 [€/kWh]	F2 [€/kWh]	F1 [€/kWh]
1	0.05	0.075	0.1125
2	0.067	0.1	0.15
3	0.08	0.12	0.18
4	0.095	0.1425	0.214

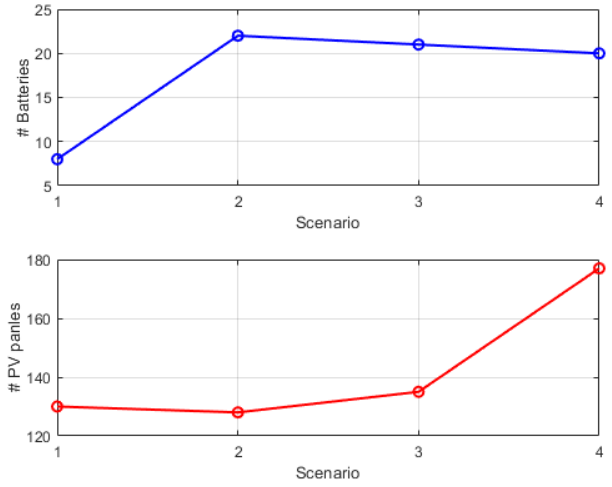

FIGURE 16. Decision variables for electricity price variations.

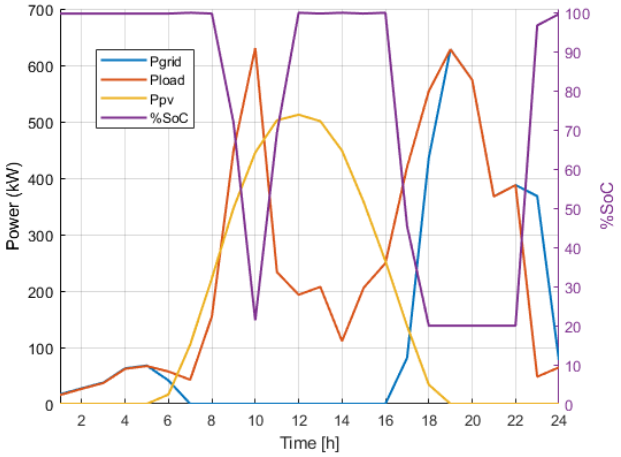

FIGURE 17. PV, EV load, grid power, and SoC of BESS per hour in one weekday.

batteries. Instead, scenario 1 represents a particular situation in which the number of installed batteries is much lower than in scenario 2 (8 units against 22) and the number of PV panels slightly higher (130 vs 128). In this scenario, the flow of energy of the different components on a weekday is shown in FIG. 17. Since the number of batteries is lower in the time interval between 8-10 h, the overall ESS is completely discharged. Then it is recharged at 100% of SoC with the solar energy coming from the panels. The optimal configuration found in scenario 1 allows, as the other scenarios, to not purchase electricity from the grid in the interval 7-17 h.

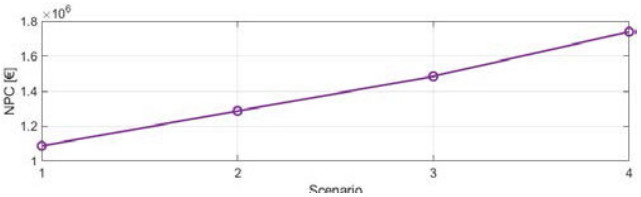

FIGURE 18. NPC for electricity price variations.

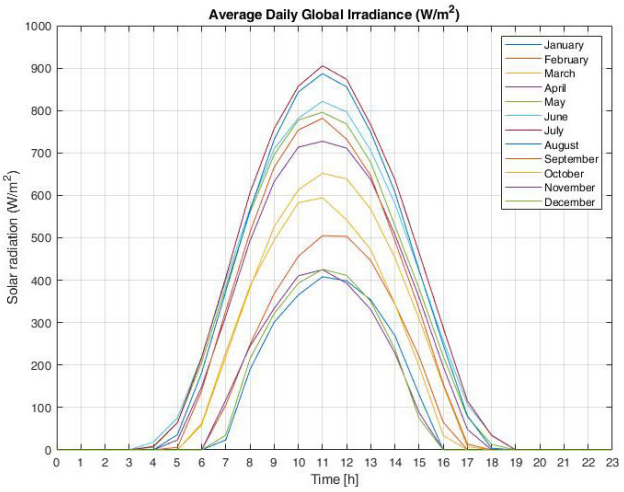

FIGURE 19. Average daily global irradiance throughout the year.

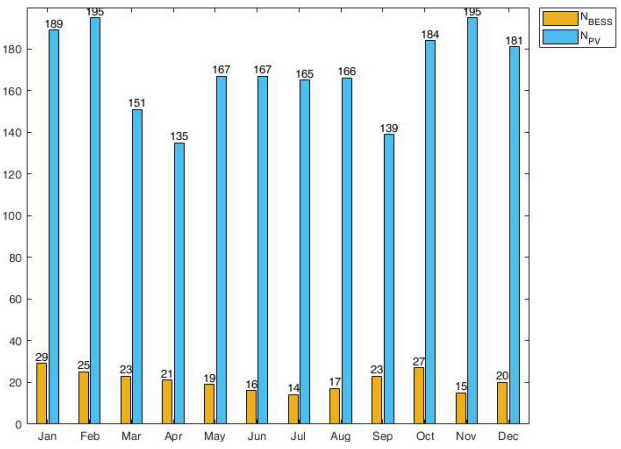

FIGURE 20. Decision variables for irradiance variations.

The trend of the NPC for the electricity prices variation, reported in FIG. 18, is very clear and as expected it linearly increases as the prices of electricity rise. An almost doubling of the electricity prices corresponds to a 60% increase in the NPC of the station.

4) SOLAR IRRADIANCE

Solar irradiance is a measure of how much solar power the photovoltaic system is producing in the installed location. As shown in FIG. 19, this irradiance varies throughout the year depending on the seasons. It also varies throughout the day, depending on the position of the sun in the sky, and

the weather. To consider the randomness of solar energy generation the average daily solar irradiance in the 12 months has been considered as input to the optimization algorithm. In FIG. 20 the results of the decision variables are depicted for all 12 months of the year.

VI. CONCLUSION

In this study, the optimal size of a PV/battery ultra-fast charging station was analyzed. First, the electric vehicles power demand of such a type of station was simulated dynamically through a probabilistic approach that took into considerations not only the random behavior of electric vehicles but also their stochastic characteristics. Then, the mathematical model of each component was developed to evaluate the optimal number of PV modules and batteries. The optimization problem employed a bi-objective function which included the net present cost of the station and its environmental impact. The multi-objective function was then reduced to a single-objective problem through the weighted sum method and finally, it was solved with genetic algorithm implemented in MATLAB. The proposed model was applied to a case study of a charging station to be installed along the Italian highway. The analysis revealed that the integration of RES and ESS in the station can bring both economic and environmental benefits. Depending on the weight factor given to the two aspects the annualized cost and the emissions can be decreased to a maximum of 55% and 50%, respectively. Finally, a sensitivity analysis is performed and from the results, it can be seen that the most influential factor on the station configuration is the electric vehicles penetration level, and hence, the vehicle demand profile, which depends not only on the penetration level but also on the electric vehicles battery capacities and categories. Indeed, if the penetration level of electric vehicles doubles and 60% of these have large battery capacities then the number of required PV panels increases of about 80% and the necessary BESS capacity doubles too.

In this work, the weighted sum method and genetic algorithm were used to solve the bi-objective function. However, many optimization techniques and algorithms can be applied in multi-objective optimization problems. Therefore, in future works, other solving methods such as Multi-Objective Particle Swarm Optimization and Mixed Integer Linear Programming will be tested to then perform a comparative analysis on the accuracy of the results of the study and the computation time. Moreover, since in this study a counter of the charging/discharging cycles of the battery as well as…has not been taken into account its model, future works can focus on the introduction of battery degradation and replacement cost in the overall analysis.

REFERENCES

[1] S. Brown, D. Pyke, and P. Steenhof, "Electric vehicles: The role and importance of standards in an emerging market," *Energy Policy*, vol. 38, no. 7, pp. 3797–3806, Jul. 2010, doi: 10.1016/J.ENPOL.2010.02.059.

[2] C. Liu, K. T. Chau, D. Wu, and S. Gao, "Opportunities and challenges of vehicle-to-home, vehicle-to-vehicle, and vehicle-to-grid technologies," *Proc. IEEE*, vol. 101, no. 11, pp. 2409–2427, Nov. 2013, doi: 10.1109/JPROC.2013.2271951.

[3] C. C. Chan, "The state of the art of electric, hybrid, and fuel cell vehicles," *Proc. IEEE*, vol. 95, no. 4, pp. 704–718, Apr. 2007, doi: 10.1109/JPROC.2007.892489.

[4] Statista. *Italy: EV Normal Power Charging Points 2015–2020*. Accessed: May 25, 2021. [Online]. Available: https://www.statista.com/statistics/906420/number-of-normal-power-charging-positions-in-italy/

[5] H. Tu, H. Feng, S. Srdic, and S. Lukic, "Extreme fast charging of electric vehicles: A technology overview," *IEEE Trans. Transport. Electrific.*, vol. 5, no. 4, pp. 861–878, Dec. 2019, doi: 10.1109/TTE.2019.2958709.

[6] M. Aryanezhad, E. Ostadaghaee, and M. Joorabian, "Management and coordination charging of smart park and V2G strategy based on Monte Carlo algorithm," in *Proc. Smart Grid Conf. (SGC)*, Dec. 2014, pp. 1–8, doi: 10.1109/SGC.2014.7090887.

[7] P. Ducharme and C. Kargas, "Feasibility of a pan-Canadian network of DC fast charging stations for EVs," in *Proc. 29th Int. Electr. Veh. Symp. (EVS)*, vol. 8, 2016, pp. 1–13.

[8] M. Moradzadeh and M. M. A. Abdelaziz, "A new MILP formulation for renewables and energy storage integration in fast charging stations," *IEEE Trans. Transport. Electrific.*, vol. 6, no. 1, pp. 181–198, Mar. 2020, doi: 10.1109/TTE.2020.2974179.

[9] W. Zhang, A. Maleki, M. A. Rosen, and J. Liu, "Sizing a stand-alone solar-wind-hydrogen energy system using weather forecasting and a hybrid search optimization algorithm," *Energy Convers. Manage.*, vol. 180, pp. 609–621, Jan. 2019, doi: 10.1016/j.enconman.2018.08.102.

[10] S. C. Raja, N. M. V. Kumar, J. S. Kumar, and J. J. D. Nesamalar, "Enhancing system reliability by optimally integrating PHEV charging station and renewable distributed generators: A bi-level programming approach," *Energy*, vol. 229, Aug. 2021, Art. no. 120746, doi: 10.1016/j.energy.2021.120746.

[11] H. Yang, Z. Wei, and L. Chengzhi, "Optimal design and techno-economic analysis of a hybrid solar–wind power generation system," *Appl. Energy*, vol. 86, no. 2, pp. 163–169, Feb. 2009, doi: 10.1016/j.apenergy.2008.03.008.

[12] B. Sun, "A multi-objective optimization model for fast electric vehicle charging stations with wind, PV power and energy storage," *J. Cleaner Prod.*, vol. 288, Mar. 2021, Art. no. 125564, doi: 10.1016/j.jclepro.2020.125564.

[13] X. Xu, W. Hu, D. Cao, Q. Huang, C. Chen, and Z. Chen, "Optimized sizing of a standalone PV-wind-hydropower station with pumped-storage installation hybrid energy system," *Renew. Energy*, vol. 147, pp. 1418–1431, Mar. 2020, doi: 10.1016/J.RENENE.2019.09.099.

[14] M. R. Mozafar, M. H. Moradi, and M. H. Amini, "A simultaneous approach for optimal allocation of renewable energy sources and electric vehicle charging stations in smart grids based on improved GA-PSO algorithm," *Sustain. Cities Soc.*, vol. 32, pp. 627–637, Jul. 2017, doi: 10.1016/J.SCS.2017.05.007.

[15] E. L. V. Eriksson and E. M. Gray, "Optimization of renewable hybrid energy systems—A multi-objective approach," *Renew. Energy*, vol. 133, pp. 971–999, Apr. 2019, doi: 10.1016/J.RENENE.2018.10.053.

[16] Y. Kim and S. Kim, "Forecasting charging demand of electric vehicles using time-series models," *Energies*, vol. 14, no. 5, p. 1487, 2021, doi: 10.3390/EN14051487.

[17] D. Fischer, A. Harbrecht, A. Surmann, and R. McKenna, "Electric vehicles' impacts on residential electric local profiles—A stochastic modelling approach considering socio-economic, behavioural and spatial factors," *Appl. Energy*, vols. 233–234, pp. 644–658, Jan. 2019, doi: 10.1016/J.APENERGY.2018.10.010.

[18] Å. L. Sørensen, K. B. Lindberg, I. Sartori, and I. Andresen, "Analysis of residential EV energy flexibility potential based on real-world charging reports and smart meter data," *Energy Buildings*, vol. 241, Jun. 2021, Art. no. 110923, doi: 10.1016/J.ENBUILD.2021.110923.

[19] M. Muratori, "Impact of uncoordinated plug-in electric vehicle charging on residential power demand," *Nature Energy*, vol. 3, no. 3, pp. 193–201, Mar. 2018, doi: 10.1038/S41560-017-0074-Z.

[20] M. Gilleran, E. Bonnema, J. Woods, P. Mishra, I. Doebber, C. Hunter, M. Mitchell, and M. Mann, "Impact of electric vehicle charging on the power demand of retail buildings," *Adv. Appl. Energy*, vol. 4, Nov. 2021, Art. no. 100062, doi: 10.1016/J.ADAPEN.2021.100062.

[21] J. Van Roy, N. Leemput, F. Geth, J. Buscher, R. Salenbien, and J. Driesen, "Electric vehicle charging in an office building microgrid with distributed energy resources," *IEEE Trans. Sustain. Energy*, vol. 5, no. 4, pp. 1389–1396, Oct. 2014, doi: 10.1109/TSTE.2014.2314754.

[22] K. Yunus, H. Z. De La Parra, and M. Reza, "Distribution grid impact of plug-in electric vehicles charging at fast charging stations using stochastic charging model," in *Proc. 14th Eur. Conf. Power Electron. Appl.*, Birmingham, U.K., 2011, pp. 1–11.
[23] L. Longo, "Optimal design of an EV fast charging station coupled with storage in Stockholm," KTH Ind. Eng. Manage., Division Energy Climate Stud., 2017.
[24] G. Celli, G. G. Soma, F. Pilo, F. Lacu, S. Mocci, and N. Natale, "Aggregated electric vehicles load profiles with fast charging stations," in *Proc. Power Syst. Comput. Conf.* Piscataway, NJ, USA: Institute of Electrical and Electronics Engineers, Aug. 2014, pp. 1–7, doi: 10.1109/PSCC.2014.7038402.
[25] E. Chiodo, D. Iannuzzi, F. Mottola, M. Pagano, and D. Proto, "A probabilistic approach to assess the requirements of an ultra-fast PEV charging station in extra-urban contexts," in *Proc. AEIT Int. Annu. Conf. (AEIT)*, Sep. 2019, pp. 1–6, doi: 10.23919/AEIT.2019.8893357.
[26] A. S. Mussa, A. Liivat, F. Marzano, M. Klett, B. Philippe, C. Tengstedt, G. Lindbergh, K. Edström, R. W. Lindström, and P. Svens, "Fast-charging effects on ageing for energy-optimized automotive $LiNi_{1/3}Mn_{1/3}Co_{1/3}O_2$/graphite prismatic lithium-ion cells," *J. Power Sources*, vol. 422, pp. 175–184, May 2019, doi: 10.1016/j.jpowsour.2019.02.095.
[27] L. Wang, Z. Qin, T. Slangen, P. Bauer, and T. van Wijk, "Grid impact of electric vehicle fast charging stations: Trends, standards, issues and mitigation measures—An overview," *IEEE Open J. Power Electron.*, vol. 2, pp. 56–74, 2021, doi: 10.1109/OJPEL.2021.3054601.
[28] *Report Periodici Delle Singole Stazioni*. Accessed: May 3, 2021. [Online]. Available: https://www.stradeanas.it/it/le-strade/osservatorio-del-traffico/report-periodici-singole-stazioni
[29] S. Guner and A. Ozdemir, "Distributed storage capacity modelling of EV parking lots," in *Proc. 9th Int. Conf. Electr. Electron. Eng. (ELECO)*, Nov. 2015, pp. 359–363, doi: 10.1109/ELECO.2015.7394580.
[30] S. Qian, X. Zhang, C. Chen, H. Wang, J. Guo, and Y. Xu, "Ageing evaluation of the distribution transformer under varying load due to electric vehicle charging," in *Proc. Int. Conf. Electr. Mater. Power Equip. (ICEMPE)*, Apr. 2021, pp. 1–4, doi: 10.1109/ICEMPE51623.2021.9509233.
[31] C. Leone and M. Longo, "Modular approach to ultra-fast charging stations," *J. Electr. Eng. Technol.*, vol. 16, no. 4, pp. 1971–1984, Jul. 2021, doi: 10.1007/S42835-021-00757-X.
[32] Fastned. *Fast Charging*. Accessed: May 13, 2021. [Online]. Available: https://fastnedcharging.com/en/how-it-works
[33] Q. Dai, J. Liu, and Q. Wei, "Optimal photovoltaic/battery energy storage/electric vehicle charging station design based on multi-agent particle swarm optimization algorithm," *Sustainability*, vol. 11, no. 7, p. 1973, Apr. 2019, doi: 10.3390/su11071973.
[34] M. H. Amrollahi and S. M. T. Bathaee, "Techno-economic optimization of hybrid photovoltaic/wind generation together with energy storage system in a stand-alone micro-grid subjected to demand response," *Appl. Energy*, vol. 202, pp. 66–77, Sep. 2017, doi: 10.1016/j.apenergy.2017.05.116.
[35] S. Ponce-Alcántara, J. P. Connolly, G. Sánchez, J. M. Míguez, V. Hoffmann, and R. Ordás, "A statistical analysis of the temperature coefficients of industrial silicon solar cells," *Energy Proc.*, vol. 55, pp. 578–588, Jan. 2014, doi: 10.1016/j.egypro.2014.08.029.
[36] A. Hussain, V.-H. Bui, J.-W. Baek, and H.-M. Kim, "Stationary energy storage system for fast EV charging stations: Simultaneous sizing of battery and converter," *Energies*, vol. 12, no. 23, p. 4516, Nov. 2019, doi: 10.3390/EN12234516.
[37] D. Sbordone, I. Bertini, B. Di Pietra, M. C. Falvo, A. Genovese, and L. Martirano, "EV fast charging stations and energy storage technologies: A real implementation in the smart micro grid paradigm," *Electr. Power Syst. Res.*, vol. 120, pp. 96–108, Mar. 2015, doi: 10.1016/J.EPSR.2014.07.033.
[38] S. S. Sheikh, M. Anjum, M. A. Khan, S. A. Hassan, H. A. Khalid, A. Gastli, and L. Ben-Brahim, "A battery health monitoring method using machine learning: A data-driven approach," *Energies*, vol. 13, no. 14, p. 3658, 2020, doi: 10.3390/EN13143658.
[39] Z. Wei, Z. Quan, J. Wu, Y. Li, J. Pou, and H. Zhong, "Deep deterministic policy gradient-DRL enabled multiphysics-constrained fast charging of lithium-ion battery," *IEEE Trans. Ind. Electron.*, vol. 69, no. 3, pp. 2588–2598, Mar. 2022, doi: 10.1109/TIE.2021.3070514.
[40] J. Wu, Z. Wei, W. Li, Y. Wang, Y. Li, and D. U. Sauer, "Battery thermal- and health-constrained energy management for hybrid electric bus based on soft actor-critic DRL algorithm," *IEEE Trans. Ind. Informat.*, vol. 17, no. 6, pp. 3751–3761, Jun. 2021, doi: 10.1109/TII.2020.3014599.
[41] M. H. Mostafa, S. H. E. A. Aleem, S. G. Ali, Z. M. Ali, and A. Y. Abdelaziz, "Techno-economic assessment of energy storage systems using annualized life cycle cost of storage (LCCOS) and levelized cost of energy (LCOE) metrics," *J. Energy Storage*, vol. 29, Jun. 2020, Art. no. 101345, doi: 10.1016/j.est.2020.101345.
[42] S. M. Hakimi and S. M. Moghaddas-Tafreshi, "Optimal sizing of a stand-alone hybrid power system via particle swarm optimization for Kahnouj area in south-east of Iran," *Renew. Energy*, vol. 34, no. 7, pp. 1855–1862, Jul. 2009, doi: 10.1016/j.renene.2008.11.022.
[43] A. R. Brown, "A multi-objective approach to infrastructure planning in the early stages of EV introduction," Dept. Statist. Oper. Res., Univ. Politècnica Catalunya, Barcelona, Spain, 2014.
[44] R. T. Marler and J. S. Arora, "Function-transformation methods for multi-objective optimization," *Eng. Optim.*, vol. 37, no. 6, pp. 551–570, Sep. 2005, doi: 10.1080/03052150500114289.
[45] M. S. Javed, A. Song, and T. Ma, "Techno-economic assessment of a stand-alone hybrid solar-wind-battery system for a remote island using genetic algorithm," *Energy*, vol. 176, pp. 704–717, Jun. 2019, doi: 10.1016/j.energy.2019.03.131.
[46] Y. Hu, K. Qian, and H. Gao, "Design of electric vehicle charging station based on genetic algorithm," *IOP Conf. Ser., Mater. Sci. Eng.*, vol. 631, no. 5, Oct. 2019, Art. no. 052025, doi: 10.1088/1757-899X/631/5/052025.
[47] A. Dina, S. Danaila, M.-V. Pricop, and I. Bunescu, "Using genetic algorithms to optimize airfoils in incompressible regime," *INCAS Bull.*, vol. 11, no. 1, pp. 79–90, Mar. 2019, doi: 10.13111/2066-8201.2019.11.1.6.
[48] S. Statharas, Y. Moysoglou, P. Siskos, G. Zazias, and P. Capros, "Factors influencing electric vehicle penetration in the EU by 2030: A model-based policy assessment," *Energies*, vol. 12, no. 14, p. 2739, Jul. 2019, doi: 10.3390/en12142739.
[49] G. Napoli, A. Polimeni, S. Micari, G. Dispenza, and V. Antonucci, "Optimal allocation of electric vehicle charging stations in a highway network: Part 2. The Italian case study," *J. Energy Storage*, vol. 26, Dec. 2019, Art. no. 101015, doi: 10.1016/j.est.2019.101015.
[50] Statista. *Italy: Electric Vehicle Registrations by Type 2018*. Accessed: Nov. 29, 2021. [Online]. Available: https://www.statista.com/statistics/1061823/electric-vehicle-registered-in-italy-by-type/
[51] *IDTechEx: Sales of Electric Motorcycles in Europe Grew 50% y-o-y in 2020—Green Car Congress*. Accessed: Nov. 29, 2021. [Online]. Available: https://www.greencarcongress.com/2021/02/20210219-electricmotorcycles.html
[52] C. E. Thomas, "Fuel cell and battery electric vehicles compared," *Int. J. Hydrogen Energy*, vol. 34, no. 15, pp. 6005–6020, Aug. 2009, doi: 10.1016/J.IJHYDENE.2009.06.003.
[53] Q. Wang, J. Li, Y. Bu, L. Xu, Y. Ding, Z. Hu, R. Liu, Y. Xu, and Z. Qin, "Technical assessment and feasibility validation of liquid hydrogen storage and supply system for heavy-duty fuel cell truck," in *Proc. 4th CAA Int. Conf. Veh. Control Intell. (CVCI)*, Dec. 2020, pp. 555–560, doi: 10.1109/CVCI51460.2020.9338639.
[54] *Traffic Bans for Trucks in Italy in 2019*. Accessed: Nov. 29, 2021. [Online]. Available: https://trans.info/en/traffic-bans-for-trucks-in-italy-in-2019-123531
[55] European Environment Agency. *Greenhouse Gas Emission Intensity of Electricity Generation in Europe*. Accessed: Jun. 13, 2021. [Online]. Available: https://www.eea.europa.eu/data-and-maps/indicators/overview-of-the-electricity-production-3/assessment-1
[56] *Electricity Storage and Renewables: Costs and Markets to 2030*, IRENA, Abu Dhabi, United Arab Emirates, 2017.
[57] B. Nykvist and M. Nilsson, "Rapidly falling costs of battery packs for electric vehicles," *Nature Climate Change*, vol. 5, no. 4, pp. 329–332, Apr. 2015, doi: 10.1038/nclimate2564.

CAROLA LEONE was born in Monza, Italy. She received the M.S. degree in electrical engineering from the Politecnico di Milano, Milan, Italy, in 2017. She is currently pursuing the joint Ph.D. degree with the Department of Energy, Politecnico di Milano, and the Research Group in Sustainable and Renewable Electrical Technologies, University of Cádiz. Her main research interest includes charging infrastructure for electric vehicle.

MICHELA LONGO (Member, IEEE) was born in Breno, Brescia, Italy. She received the M.Sc. degree in information engineering and the Ph.D. degree in mechatronics, information, innovative technologies, and mathematical methods from the University of Bergamo, Bergamo, Italy, in 2009 and 2013, respectively. She is currently an Assistant Professor at the Department of Energy, Politecnico di Milano, Milano, Italy. Her area of research interests include electric power systems, electric traction, and mechatronics. She is a member of the Italian Group of Engineering about Railways (CIFI) and the Italian Electric Association (AEIT).

LUIS M. FERNÁNDEZ-RAMÍREZ (Senior Member, IEEE) was born in Los Barrios, Cádiz, Spain. He received the M.Sc. degree in electrical engineering from the University of Seville, Seville, Spain, in 1997, and the Ph.D. degree from the University of Cádiz, Cádiz, in 2004. From 1997 to 2000, he was with the Department of Development and Research, Desarrollos Eolicos S.A., Seville. In 2000, he joined the University of Cádiz, where he is currently an Associate Professor with the Department of Electrical Engineering and the Head of the Research Group in Sustainable and Renewable Electrical Technologies (PAIDI-TEP023). His research interests include smart grids, renewable energy, energy storage, hydrogen systems, and power converters and control.

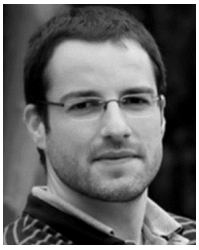

PABLO GARCÍA-TRIVIÑO was born in La Línea de la Concepción, Cádiz, Spain, in 1984. He received the B.Sc. degree in electrical engineering, the M.Sc. degree in industrial engineering, and the Ph.D. degree from the University of Cádiz, Cádiz, in 2005, 2007, and 2010, respectively. Since 2008, he has been an Associate Professor with the Department of Electrical Engineering, University of Cádiz. His current research interests include power systems and power management in hybrid systems.